IOP Conf. Series: Materials Science and Engineering **321** (2018) 012007 doi:10.1088/1757-899X/321/1/012007

Design and adaptation of a folded split ring resonator antenna for use in an animal-borne sensor

S. C. Dodson, P.G. Wiid, T.R. Niesler

Electrical & Electronic Engineering Department,University of Stellenbosch, Western Cape, South Africa

Email: sam.c.dodson@gmail.com, wiidg@sun.ac.za, trn@sun.ac.za

Abstract. We present the design, optimisation and practical evaluation of a folded split ring resonator (FSRR) antenna for the purpose of radio communication with an animal-borne sensor. We show that the measurements agree with the simulated results and that we are able to produce an electrically small antenna with low mismatch, high radiation efficiency and a quasi-isotropic radiation pattern. We then adapt the topology of the design from a circular to a rectangular shape, to completely fit inside the sensor enclosure. A quasi-isotropic pattern is maintained as well as low mismatch by appropriate tuning. There is a decrease in radiation efficiency which may be countered by a thinner substrate and retuning. We conclude that the adapted FSRR antenna is a suitable design for our application.

1. Introduction

The conservation and study of endangered wildlife can be assisted by real-time information obtained from animal-borne sensors. We consider the case of the African rhinoceros, where the sensor will be mounted on its lower back leg. For wireless communication with such a sensor, an antenna is required.

Since the sensor is a low-power device, the antenna needs to efficiently convert available power to radiated power. To realise this, the antenna should be well-matched to a $50\ \Omega$ line and internal ohmic losses should be minimised. The radiation pattern must be omnidirectional because the rhinoceros's orientation is variable. The antenna should be contained inside the sensor's enclosure, with dimensions of approximately $105\ mm \times 65\ mm \times 25\ mm$. These dimensions are much smaller than the $690\ mm$ wavelength at the operating frequency of $433\ MHz$, making the design challenging.

Little attention has been given to antenna design for tracking tags in the research literature. Usually, classic full-wave, half-wave and quarter-wave antennas are used. These radiators would not satisfy the required matching capabilities when scaled to the enclosure's dimensions. The folded split ring resonator (FSRR) antenna provides an attractive alternative for its ability to operate efficiently inside a small space, while satisfying matching, ohmic loss and pattern requirements [1]. We first consider the design of a prototype FSRR antenna based on the literature. Then we adapt the design to operate within the confines of the enclosure.

2. The folded split ring resonator antenna

The FSRR was first used as a radiator by Kim [1]. It is based on the single-arm split ring resonator which was conceived as a sub-wavelength metamaterial particle and has now seen extensive use as an electrically small antenna [2]. According to its definition, an electrically small antenna (ESA) fits inside its near-field [3]. The near-field radius for an ESA is given by the radianlength, $rl = \frac{\lambda}{2\pi}$, with λ the wavelength at the operating frequency [4]. This is also the inverse of the free-space wave number $k = \frac{2\pi}{\lambda}$. An ESA's size is typically given relative to the radianlength by the ratio $\frac{a}{rl} = ka$ with a the radius of the smallest fictitious sphere that totally encloses the antenna. ka is the antenna's electrical size.

The FSRR is depicted in figure 1. The radiation resistance R_{rad} (included in the total antenna input resistance R_{in}) and resonant frequency f_{res} decrease with smaller electrical size, hence an ESA will typically show high mismatch [5]. This is partly overcome by the folded conductor arms of the FSRR antenna which increase the input impedance Z_{in} by a factor of approximately four (compared to a single conductor) when the conductor widths are equal [6]. By raising the conductor width ratio $\frac{W_2}{W_1}$ above unity Z_{in} may be raised further. Additionally, the resonant frequency f_{res} may be lowered by decreasing the gap length GL. Both tuning mechanisms allow flexible antenna miniaturisation.

The FSRR antenna produces a quasi-isotropic radiation pattern. This behaviour may be interpreted by an even-odd mode current analysis [1]. The curved red arrows in figure 1 represent the positions of the maximum in-phase even mode currents, which form a y-directed electric dipole. The curved blue arrows represent the equal amplitude, in-phase odd-mode currents which form a z-directed magnetic dipole. The superposition of these two modes produces the quasi-isotropic pattern.

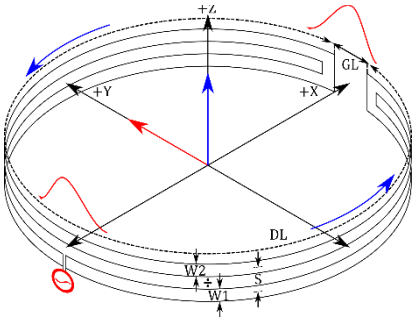

Figure 1. The FSRR antenna and its parameters.

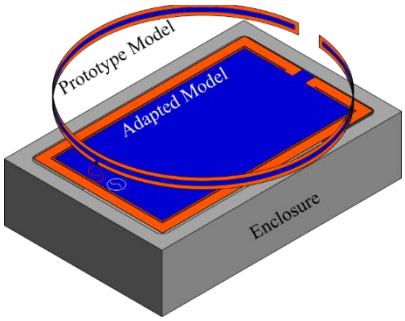

Figure 2. The first prototype and adapted prototype superimposed over the enclosure.

3. Optimisation and construction

A first prototype FSRR antenna was designed for performance validation. This was achieved using the computational electromagnetic software, FEKO. It was optimised to realise a $50\ \Omega$ input impedance on $0.2\ mm$ thick FR-4 substrate, with permittivity $\epsilon_r = 4.6$ and loss tangent $tan\delta = 0.017$. The gap length GL, dipole length DL, conductor width W (where both conductor widths were kept equal) and spacing S were optimised; their values may be seen to the left in table 1. The resulting electrical size is $ka = 0.48$, confirming that it is an ESA. Despite the small electrical size, the optimised prototype was too large to fit inside the enclosure. To adapt the model, it was flattened onto a rigid substrate and converted to a rectangular shape, as shown in figure 2. The antenna length TL is 305.87 mm as measured through the centre of the conductors. The shorter length, together with the shorter current path taken due to the sharp corners of the rectangle, causes f_{res} to increase from $435.5\ MHz$ to $471.4\ MHz$. R_{in} also decreases from $45.91\ \Omega$ to $32.63\ \Omega$. The electrical size of $ka = 0.55$ is larger than the first prototype's, but the adapted antenna's shape fits in the enclosure, regardless. To lower f_{res} the gap length was decreased from $10.4\ mm$ to $6\ mm$. For manufacturing reasons, the $0.2\ mm$ thick substrate was increased to $1.5\ mm$, which further lowered f_{res}. The conductor ratio W_2/W_1 was increased to 56.67 to raise R_{in} to $50\ \Omega$ at f_{res}. The parameters are shown to the right in table 1.

The first constructed prototype is shown in figure 3 (a). The flexible substrate made it difficult to construct accurately. It also required the construction of a large $\lambda/4$ sleeve balun [7]. The rigid substrate of the adapted prototype, shown in figure 3 (b), solved these issues. A small surface mount balun replaced the sleeve balun. The adapted prototype could also be machined to a much higher accuracy. The adapted feed was designed to face inward so that the sensor electronics could potentially be incorporated onto the substrate.

Table 1. Parameters of the first prototype and adapted prototype FSRR antennas.

First Prototype				***Adapted Prototype***				
DL (mm)	GL (mm)	W(mm)	S (mm)	TL (mm)	GL (mm)	W_1 (mm)	W_2 (mm)	S (mm)
315.8	10.40	1.38	3.53	305.87	6	0.72	40.8	2.66

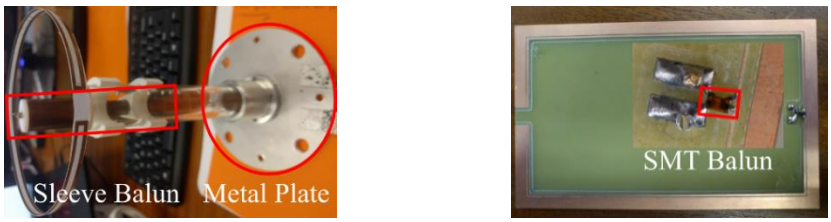

(a) (b)

Figure 3. Constructed FSRR antennas: (a) the first prototype with the sleeve balun and metal plate highlighted in red and (b) the adapted prototype with the SMT balun highlighted in red.

4. Results

The aim of the first prototype was to determine whether the FSRR antenna could meet the project requirements. It would then serve as a benchmark for the adapted prototype. The adapted prototype should maintain the performance of the original, where possible. The measured and simulated S_{11} values of the first prototype are shown in figure 4 (a). The traces align closely, confirming the accuracy of the simulated model. The minimum S_{11} value of the measured model is $-17.44\,dB$ at $436.5\,MHz$. This is a good match to a $50\,\Omega$ line. At the same frequency the simulated radiation efficiency e_{rad} (which could not be measured for the first prototype) is 95.76% and hence internal losses are small.

The adapted prototype S_{11} traces are shown in figure 4 (b). The minimum value is $-19.77\,dB$ at $433.5\,MHz$, which is lower than the original prototype. This low value is expected, given that GL and $\frac{W_2}{W_1}$ were modified. It is suspected that the increased deviation between measured and simulated traces is because of the inner feed, which is not modelled accurately in FEKO. The difference between the minimum S_{11} values is $4.5\,MHz$, which can be accounted for in the design process. The measured e_{rad} is 61.04%, compared to the simulated 77.46%, which is much lower than the e_{rad} of the first prototype. It is caused by the increased substrate thickness. The e_{rad} may be increased by decreasing the thickness and reducing GL to compensate for the higher f_{res}.

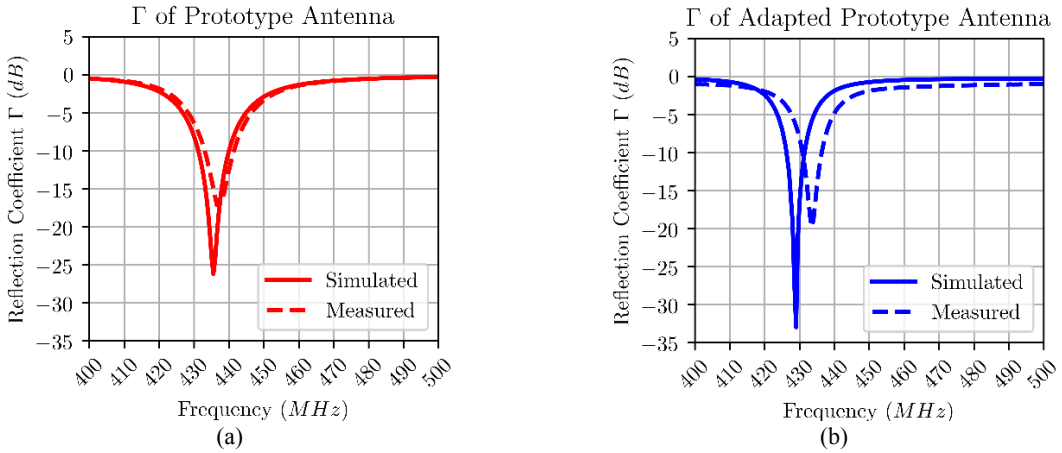

(a) (b)

Figure 4. Reflection coefficient plots of (a) the simulated first prototype FSRR versus the constructed model and (b) the simulated adapted FSRR prototype versus the constructed model.

Pattern measurements were conducted inside an anechoic chamber using a spherical near-field scanner. The antenna under test is obstructed for the positions $90° < \theta < 270°$. This corresponds to

the lower portion of the polar plots which will be ignored. A metal plate was used to mount both antennas in the chamber, the plate is shown in figure 3 (a). The plate is sturdy and was designed for larger antennas. However, it leads to scattering and a plastic plate will be used for small antennas in the future.

The total directivity polar plots for the first configuration are shown in figure 5. The simulated model with no plate present is given by the solid trace. The pattern is quasi-isotropic with a maximum directivity of $1.26\ dBi$ toward $\theta = 90°$ in the XZ plane. The measured trace is dashed and the effect of the plate is noticeable; it reinforces the pattern toward $\theta = 60°$ and $300°$ while lowering it toward $\theta = 0°$. By including the plate in the simulation (dash-dotted trace), better agreement is obtained. We conclude that, without the plate, the antenna will radiate as predicted by the initial simulation.

The adapted prototype retained a similar main current path compared to the first prototype, hence it was speculated that the quasi-isotropic pattern would be maintained. This is confirmed by figure 5 (c) and figure 5 (d) which show the adapted model polar plots. The maximum directivity is in the same direction and is lowered slightly to $1.11\ dBi$.

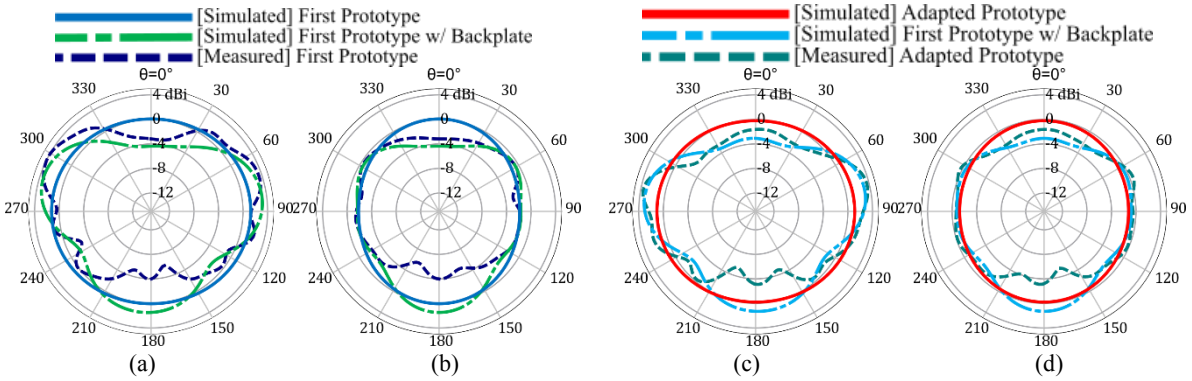

Figure 5. Far-field total directivity polar plots of measured and simulated antenna (at frequencies corresponding to their lowest S_{11} values), simulations with and without a 'plate', for (a) XZ plane first prototype; (b) YZ plane first prototype; (c) XZ plane adapted prototype; (d) YZ plane adapted prototype.

5. Conclusion & Future Work

An electrically small adapted prototype FSRR antenna of $ka = 0.55$ was designed, which satisfies most of the performance parameters and fits inside a sensor enclosure. It followed from an optimised first prototype, which satisfied the performance parameters, but was too large. The adapted model achieved a lower S_{11} value of $-19.77\ dB$ while retaining a quasi-isotropic radiation pattern. The adapted model is easier to manufacture and its inward-facing feed allows potential placement of sensor electronics on its substrate. The adapted prototype's measured e_{rad} of 61.04% is less than the simulated e_{rad} of the first prototype. However, this may easily be increased by using a thinner substrate and by decreasing the gap length. Future prototypes will analyse the effects of adding electronics to the substrate. A thinner dielectric will be used to increase radiation efficiency, and the antenna will be placed within the enclosure where its impedance characteristics will be measured.

References

[1] Kim J-H and Nam S 2017 A compact quasi-isotropic antenna based on folded split ring resonators *IEEE Antennas Wireless Propagation Lett.* **16** 294–97
[2] Dong Y and Itoh T 2012 Metamaterial-based antennas *Proc. IEEE* vol 100 pp 2271–85
[3] McLean J S 1996 A re-examination of the fundamental limits on the radiation q of electrically small antennas *IEEE Trans. Antennas Propagation* **44** 672–76
[4] Wheeler H A 1947 Fundamental limitations of small antennas *Proc. I.R.E.* vol 35 pp 1479–88
[5] Wheeler H A 1959 The radiansphere around a small antenna *Proc. IRE* vol 47 p 1325
[6] Balanis C A 2005 *Antenna theory: analaysis and design, 3rd ed.* (New Jersey: Wiley-Interscience) pp 517-15
[7] Saario S A, Lu J W and Thiel D V 2002 Full-wave analysis of choking characteristics of sleeve balun on coaxial cables *Electronics Letters* **38** pp 304-05